



**HAL**  
open science

## Time-Kill Analysis of Canine Skin Pathogens: A Comparison of Pradofloxacin and Marbofloxacin

Stefano Azzariti, Andrew Mead, Pierre-Louis Toutain, Ross Bond, Ludovic Pelligand

► **To cite this version:**

Stefano Azzariti, Andrew Mead, Pierre-Louis Toutain, Ross Bond, Ludovic Pelligand. Time-Kill Analysis of Canine Skin Pathogens: A Comparison of Pradofloxacin and Marbofloxacin. *Antibiotics*, 2023, 12 (10), pp.1548. 10.3390/antibiotics12101548 . hal-04522061

**HAL Id: hal-04522061**

**<https://hal.inrae.fr/hal-04522061>**

Submitted on 26 Mar 2024

**HAL** is a multi-disciplinary open access archive for the deposit and dissemination of scientific research documents, whether they are published or not. The documents may come from teaching and research institutions in France or abroad, or from public or private research centers.

L'archive ouverte pluridisciplinaire **HAL**, est destinée au dépôt et à la diffusion de documents scientifiques de niveau recherche, publiés ou non, émanant des établissements d'enseignement et de recherche français ou étrangers, des laboratoires publics ou privés.



Distributed under a Creative Commons Attribution 4.0 International License

## Article

# Time-Kill Analysis of Canine Skin Pathogens: A Comparison of Pradofloxacin and Marbofloxacin

Stefano Azzariti <sup>1</sup> , Andrew Mead <sup>1</sup>, Pierre-Louis Toutain <sup>1,2</sup>, Ross Bond <sup>3</sup> and Ludovic Pelligand <sup>1,3,\*</sup> 

<sup>1</sup> Department of Comparative Biomedical Sciences, Royal Veterinary College, Hawkshead Lane, North Mymms, Hatfield AL9 7TA, UK; sazzariti@rvc.ac.uk (S.A.); amead@rvc.ac.uk (A.M.); pltoutain@rvc.ac.uk (P.-L.T.)

<sup>2</sup> INHERES, Université de Toulouse, INRAE, Ecole Nationale Vétérinaire de Toulouse, 23 Chemin des Capelles-BP 87614, CEDEX 03, 31076 Toulouse, France

<sup>3</sup> Department of Clinical Sciences and Services, Royal Veterinary College, Hawkshead Lane, North Mymms, Hatfield AL9 7TA, UK; rbond@rvc.ac.uk

\* Correspondence: lpelligand@rvc.ac.uk

**Abstract:** Time-kill curves (TKCs) are more informative compared with the use of minimum inhibitory concentration (MIC) as they allow the capture of bacterial growth and the development of drug killing rates over time, which allows to compute key pharmacodynamic (PD) parameters. Our study aimed, using a semi-mechanistic mathematical model, to estimate the best pharmacokinetic/pharmacodynamic (PK/PD) indices ( $fAUC/MIC$  or  $\%fT > MIC$ ) for the prediction of clinical efficacy of veterinary FQs in *Staphylococcus pseudintermedius*, *Staphylococcus aureus*, and *Escherichia coli* collected from canine pyoderma cases with a focus on the comparison between marbofloxacin and pradofloxacin. Eight TKCs for each bacterial species (4 susceptible and 4 resistant) were analysed in duplicate. The best PK/PD index was  $fAUC_{24h}/MIC$  in both staphylococci and *E. coli*. For staphylococci, values of 25–40 h were necessary to achieve a bactericidal effect, whereas the calculated values (25–35 h) for *E. coli* were lower than those predicting a positive clinical outcome (100–120 h) in murine models. Pradofloxacin showed a higher potency (lower  $EC_{50}$ ) in comparison with marbofloxacin. However, no difference in terms of a maximal possible pharmacological killing rate ( $E_{max}$ ) was observed. Taking into account in vivo exposure at the recommended dosage regimen (3 and 2 mg/kg for pradofloxacin and marbofloxacin, respectively), the overall killing rates ( $K_{drug}$ ) computed were also similar in most instances.

**Keywords:** canine pyoderma; *Staphylococcus* spp.; *Escherichia coli*; fluoroquinolones; MIC; mathematical modelling; semi-mechanistic model; PK/PD index; dose fractionation; resistance



**Citation:** Azzariti, S.; Mead, A.; Toutain, P.-L.; Bond, R.; Pelligand, L. Time-Kill Analysis of Canine Skin Pathogens: A Comparison of Pradofloxacin and Marbofloxacin. *Antibiotics* **2023**, *12*, 1548. <https://doi.org/10.3390/antibiotics12101548>

Academic Editor: Carlos M. Franco

Received: 20 September 2023

Revised: 10 October 2023

Accepted: 13 October 2023

Published: 17 October 2023



**Copyright:** © 2023 by the authors. Licensee MDPI, Basel, Switzerland. This article is an open access article distributed under the terms and conditions of the Creative Commons Attribution (CC BY) license (<https://creativecommons.org/licenses/by/4.0/>).

## 1. Introduction

The use of minimum inhibitory concentrations (MICs) is pivotal in the evaluation of the pharmacodynamics (PD) of antimicrobials. Its measurement has been standardised, and the clinical breakpoints are the MIC values that allow the interpretation of antimicrobial susceptibility tests (ASTs) [1]. Nevertheless, MICs have limitations as these values represents a single terminal observation at about 24 h after initiation of the test, and these data do not inform on the time course of the bacterial count from an initial inoculum [2–5].

Time-kill curves (TKCs) or time-kill assays are more informative and quantify the chronological change in bacterial populations from a standardized initial inoculum exposed to one or multiple MICs. The antibiotic effect is measured in relation to growth and death of bacteria over time and is not only a snapshot of a single antimicrobial drug (AMD) concentration with its net effect [6,7]. For TKCs, a given bacterial inoculum can be exposed either to a static nominal antibiotic concentration or to concentrations that vary over time (dynamic time-kill curves, e.g., hollow fibre infection model) [8].

The PD-based informative value of TKCs can be revealed by mathematical modelling, which consists of linking bacterial exposure to an antibiotic concentration (constant or

variable) to an observed effect through a pharmacokinetic/pharmacodynamic (PK/PD) model. The classical PD model is the  $E_{\max}$  model, which allows the estimation of two genuine PD parameters separately: a maximum possible effect noted as  $E_{\max}$  and the antibiotic concentration giving an effect equal to  $E_{\max}/2$  noted as  $EC_{50}$  (effective 50% concentration).  $E_{\max}$  is a measure of antibiotic pharmacological efficacy, and  $EC_{50}$  is a measure of antibiotic potency. A more advanced model is the Hill model; that is, the  $E_{\max}$  model with a supplementary parameter ( $\gamma$ ) describing the slope of a sigmoidal concentration-effect curve, thus reflecting the steepness or sensitivity of the concentration-effect relationship [9].

Mathematical modelling of time-kill curve data also provides useful insight into the selection of the best PK/PD index to predict clinical efficacy, e.g.,  $fAUC/MIC$  or  $\%fT > MIC$  (with  $f$  indicating the free concentration of the antimicrobial drug used for computation). These two PK/PD indices combine drug exposure and MIC values with the drug-related response over time and at specific time points [8]. The advantage of the *in silico* method also relies on the replacement of experimental animals, such rodents, for dose fractionation studies [10]. PD and PK data can be integrated from independent (or the same) studies, with the aim to administer a dose that achieves a plasma concentration able to reach or exceed an average free plasma concentration that equals the MIC ( $fAUC/MIC$ ) or to achieve a free plasma concentration above the MIC for a given fraction of the dosing interval ( $\%fT > MIC$ ).

Several research groups have proposed frameworks for more advanced mathematical modelling of antimicrobial drugs on bacterial populations using semi-mechanistic PK/PD models. These combine biological and mechanistic knowledge, where observed data guide the model structure and parameter estimates. Models describe (1) bacterial growth and natural death, (2) drug effects, (3) regrowth and resistance emergence, and (4) antibiotic combinations and their interactions [8]. These models have been implemented in veterinary medicine [7,11,12]. With regard to veterinary fluoroquinolones (FQs) and canine skin pathogens, different studies have evaluated their killing effects in comparison with other antimicrobial classes using standard kill curves without modelling [13,14] or a simple inhibitory  $I_{\max}$  model using only the final bacterial counts at 24 h [15]. Moreover, *in vitro* dynamic studies showed that at concentrations associated with standard oral doses of marbofloxacin (2 mg/kg) and pradofloxacin (3 mg/kg), a higher and more sustained bactericidal effect was observed with pradofloxacin [16].

Accordingly, the objective of our study was to (1) implement a semi-mechanistic mathematical model to time-kill analysis, (2) to estimate bacterial growth parameters and PD parameters, and (3) obtain the best PK/PD indices for the prediction of clinical efficacy of two veterinary FQs against three bacterial species, namely *S. aureus*, *S. pseudintermedius*, and *E. coli*, through dose-fractionation studies.

We hypothesised that (i) pradofloxacin was more potent ( $EC_{50}$  lower) and potentially more bactericidal (higher  $E_{\max}$ ) in comparison to marbofloxacin and that (ii) predicted clinical efficacy at steady-state dosing would, however, be less evident between the two FQs due to differences in plasma exposure that favour marbofloxacin due to lower plasma clearance [17,18].

## 2. Results

### 2.1. Descriptive Time-Kill Analysis

In susceptible isolates, the highest bactericidal effect (expressed as 3  $\log_{10}$  reduction), was achieved at 8 times the MIC within 4–8 h in *S. pseudintermedius* (median 8 h for marbofloxacin and 6 h for pradofloxacin), 4–24 h in *S. aureus* (median 6 h for both drugs), and 0.5–4 h in *E. coli* (1.25 h for marbofloxacin and 1.5 h for pradofloxacin). In resistant isolates, the highest bactericidal effect was achieved at 8 times the MIC within 4–8 h for *S. pseudintermedius* (median 8 h for both drugs), 4–24 h for *S. aureus* (median of 24 h for marbofloxacin and 8 h for pradofloxacin), and 4–24 h for *E. coli* (median 7 h for marbofloxacin and 4 h for pradofloxacin).

## 2.2. Time-Kill Curve Mathematical Modelling

Semi-mechanistic models were used for the TKC analysis and modelling as proposed by Nielsen and Friberg [19] (Figure 1) for staphylococci, and Campion et al. [20] (Figure 2) for *E. coli*.

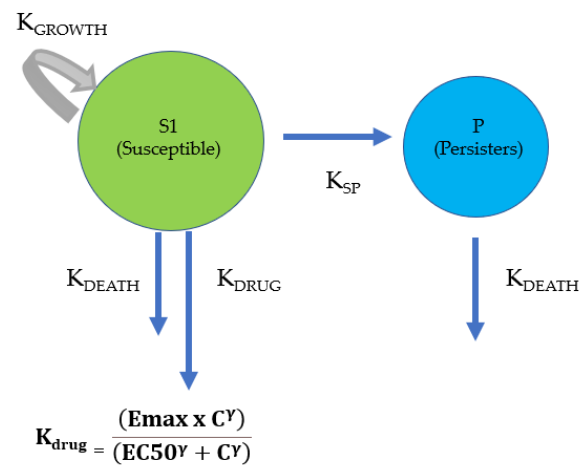


**Figure 1.** Semi-mechanistic model for TKC analysis and modelling proposed by Nielsen and Friberg [19]. The model comprises two compartments. The first compartment is “S”, which includes growing and drug-susceptible bacteria. Bacterial growth occurs at a constant rate  $K_{\text{growth}}$ . Bacterial death ( $K_{\text{death}}$ ) naturally occurs during the stationary phase due to exhaustion of nutrients, or it is accelerated by the parallel drug effect ( $K_{\text{drug}}$ ).  $E_{\text{max}}$ ,  $EC_{50}$ , and gamma are the PD parameters that describe efficacy (maximum effect achieved), potency (50% of  $E_{\text{max}}$ ), and sensitivity (steepness of the concentration-effect curve). The second compartment contains persisters (P), which are non-growing and non-drug-susceptible bacteria but eliminated according to  $K_{\text{death}}$ .  $K_{\text{SP}}$  represents the irreversible constant rate between S and P compartments.  $K_{\text{death}}$  for persisters is the same as that noted for susceptible bacteria.

### Pre-existing heterogeneous population model (Subpopulations S1, S2, P)

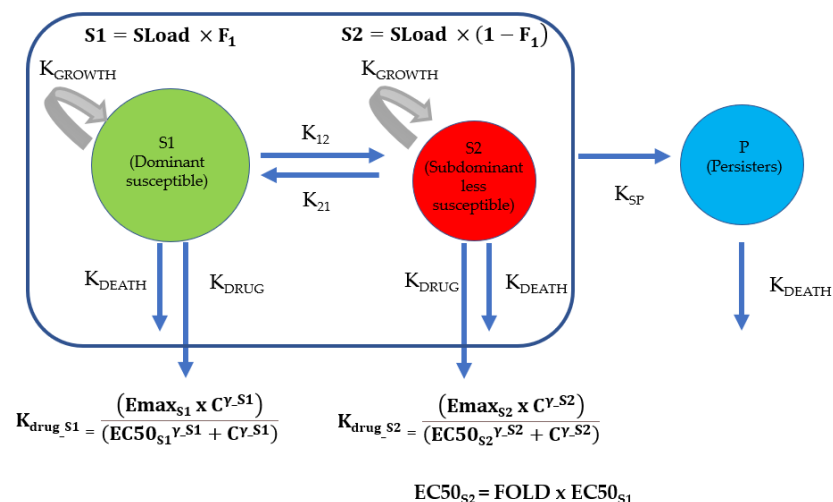


**Figure 2.** Schematic representation of pre-existing heterogeneous population model adopted for *E. coli* time-kill analysis. The model comprises 3 subpopulations: S1, S2 and P. S1 is the dominant FQ-susceptible subpopulation, whereas S2 the subdominant less FQ-susceptible subpopulation. This was either explained by spontaneous mutations in the absence of FQ or by an increase in the rate of the mutation when exposed to concentrations of FQ below or around the MIC. The S1 and S2 subpopulations have the same growth rate constant ( $K_{\text{growth}}$ ) and death rate ( $K_{\text{death}}$ ), but the drug

killing effect is influenced by their different susceptibilities ( $K_{\text{drug}_S1}$  and  $K_{\text{drug}_S2}$ ). The system was considered to be already in equilibrium during the initial exposure to FQ, and the  $K_{12}/K_{21}$  ratio was estimated by directly evaluating a distribution factor (F) of the population between the population S1 (F) and subpopulation S2 ( $1 - F$ ) with  $F = (1 - F) \times (K_{12}/K_{21})$ . The P compartment is represented by persisters, which do not grow but have a constant death rate ( $K_{\text{death}}$ ).  $K_{SP}$  is the irreversible transfer constant between S<sub>1</sub> or S<sub>2</sub> and P compartments. The potency ratio between S<sub>2</sub> and S<sub>1</sub> was estimated as  $\text{FOLD} = \text{EC}_{50S2}/\text{EC}_{50S1}$  for each drug.

Parameters relating to growth of the bacterial system were shared for both drugs and are summarized in Table 1, with drug PD parameters provided in Tables 2–4. Visual predictive check (VPC; Figures S1–S12) showed good predictability of the model with exposure of both drugs and their relative concentrations (as multiples of MICs) tested. Goodness of fit plots (PRED, IPRED, CWRES and IWRES) were appropriate (Figures S13–S15).

**Table 1.** Bacterial growth parameter estimates and confidence intervals in *S. pseudintermedius*, *S. aureus*, and *E. coli* collected from canine skin infection cases.

Bacterial Growth System Parameters <i>S. pseudintermedius</i>		Bootstrap (n = 30)		
	Estimate	Median	2.5% CI	97.5% CI
$K_{\text{GROWTHMAX}}$ ( $\text{h}^{-1}$ )	1.41	1.36	1.22	1.56
$K_{\text{DEATH}}$ ( $\text{h}^{-1}$ )	0.179		Fixed	
Alpha ( $\text{h}^{-1}$ )	0.39	0.41	0.33	0.52
$B_{\text{MAX}}$ (CFU/mL)	$6.02 \times 10^{+09}$	$6.72 \times 10^{+09}$	$5.45 \times 10^{+09}$	$8.91 \times 10^{+09}$
CV% $B_{\text{MAX}}$ (inter-strain variability)	130%			
Bacterial growth system parameters <i>S. aureus</i>		Bootstrap (n = 30)		
	Estimate	Median	2.5% CI	97.5% CI
$K_{\text{GROWTHMAX}}$ ( $\text{h}^{-1}$ )	1.36	1.36	1.23	1.50
$K_{\text{DEATH}}$ ( $\text{h}^{-1}$ )	0.179		Fixed	
Alpha ( $\text{h}^{-1}$ )	0.77	0.79	0.58	9.99
$B_{\text{MAX}}$ (CFU/mL)	$6.60 \times 10^{+09}$	$7.16 \times 10^{+09}$	$5.59 \times 10^{+09}$	$1.07 \times 10^{+10}$
CV% $B_{\text{MAX}}$ (inter-strain variability)	124%			
Bacterial growth System parameters <i>E. coli</i>		Jacobian estimate		
	Estimate	CV%	2.5% CI	97.5% CI
$K_{\text{GROWTHMAX}}$ ( $\text{h}^{-1}$ )	2.00	2.57	1.90	2.10
$K_{\text{DEATH}}$ ( $\text{h}^{-1}$ )	0.179		Fixed	
$B_{\text{MAX}}$ (CFU/mL)	$6.84 \times 10^{+09}$	15.96	$4.70 \times 10^{+09}$	$8.98 \times 10^{+09}$

$K_{\text{GROWTHMAX}}$ : maximal growth rate;  $K_{\text{death}}$ , natural death rate; Alpha, rate constant reflecting the delay required to achieve maximal steady-state growth rate;  $B_{\text{MAX}}$ , maximum possible bacterial density.

Average drug concentrations and predicted in vivo drug effects are presented in Table 5. Critical values of PK/PD index are presented in Table S6. For all dose fractionations,  $f\text{AUC}_{\text{PK}_0-24\text{h}}/\text{MIC}$  outperformed  $f\%T > \text{MIC}$  as the best PK/PD index for both FQs against either of the three bacterial species.

**Table 2.** Pharmacodynamic parameters in 4 FQ-susceptible and 4 FQ-resistant strains of *S. pseudintermedius* collected from canine pyoderma or skin wound cases.

Isolate	PRADOFLOXACIN					MARBOFLOXACIN				
	Estimates		Bootstrap ( <i>n</i> = 30)			Estimates		Bootstrap ( <i>n</i> = 30)		
	Susceptible	Resistant	Median	2.5% CI	97.5% CI	Susceptible	Resistant	Median	2.5% CI	97.5% CI
	EC <sub>50</sub> _Pradofloxacin (mg/L)					EC <sub>50</sub> _Marbofloxacin (mg/L)				
MSSP_22219	0.037	-	0.036	0.029	0.049	0.17	-	0.18	0.15	0.21
MSSP_108	0.041	-	0.041	0.032	0.054	0.49	-	0.45	0.41	0.53
MRSP_1726	0.033	-	0.039	0.030	0.054	0.18	-	0.19	0.15	0.21
MRSP_41	0.031	-	0.034	0.026	0.048	0.18	-	0.17	0.12	0.19
MSSP_98	-	0.25	0.25	0.22	0.28	-	2.63	2.79	2.58	3.06
MSSP_115	-	0.82	0.82	0.69	0.90	-	8.41	8.58	7.70	11.38
MRSP_38	-	1.49	1.72	1.46	1.84	-	19.94	22.21	19.71	32.26
MRSP_67	-	1.21	1.30	1.07	1.64	-	22.83	24.00	22.02	25.42
	E <sub>max</sub> _Pradofloxacin (h <sup>-1</sup> )					E <sub>max</sub> _Marbofloxacin (h <sup>-1</sup> )				
	2.23	-	2.36	1.74	2.87	1.85	-	1.91	1.53	2.04
	-	1.80	1.72	1.54	2.03	-	1.64	1.61	1.44	1.86
	Gamma_Pradofloxacin (scalar)					Gamma_Marbofloxacin (scalar)				
	1.90	-	1.87	1.67	2.54	2.58	-	2.58	2.30	3.01

E<sub>max</sub>, maximal increase in killing rate in addition to K<sub>DEATH</sub> (e.g., 2.23 h<sup>-1</sup> = mean constant of 27 min); EC<sub>50</sub>, concentration required to achieve 50% of E<sub>max</sub>; Gamma is the Hill's coefficient. Common E<sub>max</sub> and gamma values were estimated for the four susceptible and the four resistant isolates.

**Table 3.** Pharmacodynamic parameters in 4 FQ-susceptible and 4 FQ-resistant strains of *S. aureus* collected from canine pyoderma or skin wound cases.

Isolate	PRADOFLOXACIN					MARBOFLOXACIN				
	Estimates		Bootstrap ( <i>n</i> = 30)			Estimates		Bootstrap ( <i>n</i> = 30)		
	Susceptible	Resistant	Median	2.5% CI	97.5% CI	Susceptible	Resistant	Median	2.5% CI	97.5% CI
	EC <sub>50</sub> _Pradofloxacin (mg/L)					EC <sub>50</sub> _Marbofloxacin (mg/L)				
MSSA_476	0.061	-	0.062	0.058	0.085	0.32	-	0.317	0.297	0.359
MSSA_B98	0.072	-	0.076	0.069	0.103	0.31	-	0.31	0.29	0.36
MRSA_A53	0.051	-	0.052	0.040	0.066	0.28	-	0.28	0.26	0.32
MRSA_A54	0.031	-	0.031	0.024	0.052	0.25	-	0.25	0.22	0.28
MSSA_B53	-	1.29	1.28	1.24	1.48	-	15.47	15.74	14.78	16.85
MSSA_B94	-	1.34	1.34	1.29	1.90	-	17.05	17.77	16.15	19.16
MRSA_A009	-	1.34	1.33	1.26	1.87	-	16.30	16.72	15.53	17.65
MRSA_A69	-	4.46	4.20	4.10	5.30	-	60.60	62.30	57.22	65.31
	E <sub>max</sub> _Pradofloxacin (h <sup>-1</sup> )					E <sub>max</sub> _Marbofloxacin (h <sup>-1</sup> )				
	2.17	-	2.30	1.88	2.69	1.97	-	2.01	1.67	2.23
	Gamma_Pradofloxacin (scalar)					Gamma_Marbofloxacin (scalar)				
	2.06	-	1.98	1.14	2.68	2.34	-	2.28	1.80	2.86

E<sub>max</sub>, maximal increase in killing rate in addition to K<sub>DEATH</sub> (e.g., 2.17 h<sup>-1</sup> = mean constant of 28 min); EC<sub>50</sub>, concentration required to achieve 50% of E<sub>max</sub>; Gamma is the Hill's coefficient. Common E<sub>max</sub> and gamma values were estimated for the four susceptible and the four resistant isolates.

**Table 4.** Pharmacodynamic parameters in 4 FQ-susceptible and 4 FQ-resistant *E. coli* collected from canine pyoderma or skin wound cases.

Isolate	PRADOXIFLOXACIN					MARBOXIFLOXACIN				
	Estimates		Precision of Estimates			Estimates		Precision of Estimates		
	Susceptible	Resistant	CV%	2.5% CI	97.5% CI	Susceptible	Resistant	CV%	2.5% CI	97.5% CI
	EC <sub>50</sub> _Pradofloxacin_S1 (mg/L)					EC <sub>50</sub> _Marbofloxacin_S1 (mg/L)				
<i>E. coli</i> 14L_1510	0.047	-	8.72	0.04	0.05	0.119	-	9.01	0.10	0.14
<i>E. coli</i> 16L_1242	0.052	-	9.13	0.04	0.06	0.178	-	9.80	0.14	0.21
<i>E. coli</i> 17L_0826	0.033	-	9.43	0.03	0.04	0.157	-	9.74	0.13	0.19
<i>E. coli</i> 17L_1562	0.076	-	9.29	0.06	0.09	0.642	-	9.88	0.52	0.77
<i>E. coli</i> 2443	-	1.81	5.62	1.61	2.01	-	4.03	4.40	3.69	4.38
<i>E. coli</i> 10L_2253	-	2.07	5.88	1.83	2.30	-	7.81	3.50	7.27	8.34
<i>E. coli</i> 10L_3690	-	7.43	6.69	6.45	8.41	-	23.55	4.55	21.45	25.66
<i>E. coli</i> 15L_3275	-	13.38	5.37	11.97	14.80	-	15.91	4.43	14.53	17.29
EC <sub>50</sub> _Pradofloxacin_S2 = 1.97 × EC <sub>50</sub> _Pradofloxacin_S1 (mg/L)						EC <sub>50</sub> _Marbofloxacin_S2 = 1.67 × EC <sub>50</sub> _Marbofloxacin_S1 (mg/L)				
E <sub>max</sub> _ Pradofloxacin (h <sup>-1</sup> )						E <sub>max</sub> _Marbofloxacin (h <sup>-1</sup> )				
8.73	-	3.63	8.11	9.35	17.14	-	4.22	15.72	18.56	
-	3.11	3.03	2.93	3.30	-	2.85	2.64	2.71	3.00	
Gamma_Pradofloxacin (scalar)						Gamma_Marbofloxacin (scalar)				
1.17		5.58	1.04	1.30	1.12		3.91	1.03	1.20	
	2.37	10.08	1.90	2.84		2.80	8.22	2.35	3.25	

For both susceptible and resistant strains, the initial inoculum is homogeneous with a population noted S1 present exclusively in the inoculum ( $F = 99.999998\%$ ). Upon exposure to the FQ, a resistant population (for the 4 isolates initially susceptible) or more resistant (for the 4 isolates initially already resistant) noted S2 will emerge during the test. S2 is at the origin of the regrowth phenomenon when the tested concentrations of FQ are between the MICs of S1 and those of S2, and this dynamic is captured by the model making it possible to estimate the EC<sub>50</sub> of S1 and S2, the EC<sub>50</sub> of S2 were estimated by a multiplying factor of S1. E<sub>max</sub>, maximal increase in the killing rate in addition to K<sub>DEATH</sub> (e.g., 8.73 h<sup>-1</sup> = mean constant of 6.9 min); EC<sub>50</sub>\_S1, concentration required to achieve 50% of E<sub>max</sub> for the dominant more susceptible population S1; Gamma is the Hill's coefficient; coefficient of variation (CV%) and confidence interval (CI) are represented in the Jacobian estimate and obtained using a simple run model. FOLD is a parameter that represents the potency ratio between the EC<sub>50</sub>S2 and EC<sub>50</sub>S1.

**Table 5.** Average free plasma concentrations ( $\mu\text{g}/\text{mL}$ ) and predicted in vivo killing drug effect ( $K_{\text{drug}}$ ) after the first dose administration and at steady state. These parameters were measured after simulation of PK data obtained from free-plasma concentrations of 2 mg/kg marbofloxacin from Schneider, Thomas, Boisrame and Deleforge [18] and 3 mg/kg pradofloxacin from Hauschild, et al. [21]. With regards to marbofloxacin, 9.1% [22] and 25% (value in bold, [23]) protein binding were considered, and the corresponding average plasma concentration and  $K_{\text{drug}}$  values at the first dose and at steady state were calculated. Two representative isolates (susceptible and resistant) were chosen for each bacterial species (*S. pseudintermedius*, *S. aureus*, and *E. coli*).

Isolate	PRADOFLOXACIN					MARBOFLOXACIN				
	Average Free Plasma Concentration ( $\mu\text{g}/\text{mL}$ )			$K_{\text{drug}}$ ( $\text{h}^{-1}$ )		Average Free Plasma Concentration ( $\mu\text{g}/\text{mL}$ )			$K_{\text{drug}}$ ( $\text{h}^{-1}$ )	
	Experimental MIC ( $\mu\text{g}/\text{mL}$ )	First Dose	Steady State	First Dose	Steady State	Experimental MIC ( $\mu\text{g}/\text{mL}$ )	First Dose	Steady State	First Dose	Steady State
MSRP 41 (susceptible)	0.025			2.21	2.21	0.20			1.78/1.73	1.82/1.79
MRSP 67 (resistant)	0.9	0.45	0.51	0.24	0.29	11.2	0.61/0.51	0.83/0.68	No efficacy (0.0001/0.0001)	No efficacy (0.0003/0.0002)
MSSA B98 (susceptible)	0.056			2.12	2.14	0.4			1.64/1.50	1.79/1.70
MSSA B53 (resistant)	1.8	0.45	0.51	0.22	0.28	12.8	0.61/0.51	0.83/0.68	No efficacy (0.001/0.0006)	No efficacy (0.002/0.001)
<i>E. coli</i> 14L-1510 (susceptible)	0.0218			8.15	8.23	0.025			14.74/14.29	15.78/14.98
<i>E. coli</i> 10L-2253 (resistant)	2.8	0.45	0.51	0.081	0.11	14.4	0.61/0.51	0.83/0.68	No efficacy (0.002/0.001)	No efficacy (0.005/0.0030)



### 2.3. Time-Kill Curve Analysis

*S. pseudintermedius*: The maximal growth rate ( $K_{\text{growthmax}}$ ) was at  $1.41 \text{ h}^{-1}$ , which means that doubling the population size under the maximum growth condition requires 0.71 h or 42 min (Table 1). The natural death rate ( $K_{\text{death}}$ ), which naturally occurs in all bacterial populations at a constant rate and as a “net kill” during the stationary phase when bacteria are not growing, was fixed at  $0.179 \text{ h}^{-1}$ , corresponding to an average lifespan of 335 min for a bacterium. Alpha, the rate constant reflecting the delay required to achieve a maximal steady-state growth rate, was estimated as  $0.39 \text{ h}^{-1}$ , corresponding to an average delay of 154 min.

The median maximum bacterial density reached ( $B_{\text{max}}$ ) was  $6.02 \times 10^9 \text{ CFU/mL}$ .

The pradofloxacin-induced maximal bacterial killing rate ( $E_{\text{max}}$ ) was  $2.23 \text{ h}^{-1}$  (or equivalently a mean killing rate of 27 min) for susceptible and  $1.80 \text{ h}^{-1}$  (33 min) for resistant isolates (Table 2), which resulted in a 13.4-fold and 11.0-fold increase in the overall death rate, respectively. The marbofloxacin-induced maximal bacterial killing rate ( $E_{\text{max}}$ ) was  $1.85 \text{ h}^{-1}$  (32 min) for susceptible and  $1.64 \text{ h}^{-1}$  (36 min) for marbofloxacin-resistant isolates, which resulted in a 11.3-fold and 10.2-fold increase in the overall death rate.

For the susceptible isolates, estimates of potency  $EC_{50}$  (concentration necessary to achieve 50% of the maximal effect) ranged from 0.170 to 0.49  $\mu\text{g/mL}$  for marbofloxacin and 0.031 to 0.041  $\mu\text{g/mL}$  for pradofloxacin. For the resistant isolates, potency estimates ranged from 2.63 to 22.83  $\mu\text{g/mL}$  for marbofloxacin and 0.25 to 1.49  $\mu\text{g/mL}$  for pradofloxacin.

A high correlation was observed between the experimental and estimated MICs for both marbofloxacin ( $R^2 = 0.9536$ ) and pradofloxacin ( $R^2 = 0.9925$ ) (Figure S17).

*S. aureus*:  $K_{\text{growthmax}}$  was calculated as  $1.36 \text{ h}^{-1}$ , which yielded an average maximum growth rate of 44 min (Table 1), versus a natural death rate ( $K_{\text{death}}$ ) fixed at  $0.179 \text{ h}^{-1}$  (335 min). Alpha was estimated as  $0.77 \text{ h}^{-1}$ , which is equivalent to an average delay of 78 min.  $B_{\text{max}}$  (maximum inoculum reached) was  $6.60 \times 10^9 \text{ CFU/mL}$ .

$E_{\text{max}}$  was similar in susceptible and resistant isolates for both drugs at  $2.17 \text{ h}^{-1}$  (28 min) for pradofloxacin and  $1.97 \text{ h}^{-1}$  (30 min) for marbofloxacin, which resulted in 13.1-fold and 11.9-fold increases in the overall death rate, respectively.

For the susceptible isolates, estimates of potency  $EC_{50}$  values ranged from 0.25 to 0.31  $\mu\text{g/mL}$  for marbofloxacin and 0.031 to 0.072  $\mu\text{g/mL}$  for pradofloxacin. For the resistant isolates, potency estimates ranged from 15.47 to 60.60  $\mu\text{g/mL}$  for marbofloxacin and 1.29 to 4.46  $\mu\text{g/mL}$  for pradofloxacin (Table 3). A high correlation was observed between measured and estimated MICs for both drugs ( $R^2 = 0.9880$  marbofloxacin,  $R^2 = 0.9501$  pradofloxacin) (Figure S17).

*E. coli*: A pre-existing heterogenous population model was adopted for *E. coli* and greatly improved model fitting compared to the basic model (Figure 2). It included two initial bacterial subpopulations noted S1 (dominant susceptible) and S2 (subdominant less susceptible) (Figure 2), which can be estimated both in FQ-susceptible and FQ-resistant isolates. This was either explained by spontaneous mutations in the absence of FQ or by an increase in the rate of mutation when exposed to concentrations of FQ below or around the MIC. Alpha, the rate constant that reflects a possible growth delay of *E. coli* in the test medium, was not included in the model as no delay was observed in TKCs in comparison with staphylococci; removing this parameter was not deleterious to the model fit.

$K_{\text{growthmax}}$  was estimated as  $2.00 \text{ h}^{-1}$ , which is equivalent to an average maximum growth rate of 30 min (Table 1), versus a natural death rate ( $K_{\text{death}}$ ) fixed at  $0.179 \text{ h}^{-1}$  (335 min).  $B_{\text{max}}$  was estimated as  $6.84 \times 10^9 \text{ CFU/mL}$ . The pradofloxacin-induced maximal bacterial killing rate ( $E_{\text{max}}$ ) was  $8.73 \text{ h}^{-1}$  (6.9 min) for susceptible and  $3.11 \text{ h}^{-1}$  (19 min) for resistant bacteria (Table 4), which resulted in 49-fold and 18.4-fold increases in the overall death rate, respectively. The marbofloxacin-induced maximal bacterial killing rate ( $E_{\text{max}}$ ) was  $17.1 \text{ h}^{-1}$  (3.5 min) for susceptible and  $2.85 \text{ h}^{-1}$  (21 min) for resistant isolates, which resulted in 96.0-fold and 16.9-fold increases in the overall death rate, respectively.

For the susceptible isolates, estimates of potency for S1 ( $EC_{50}$ ) ranged from 0.033 to 0.076  $\mu\text{g/mL}$  for pradofloxacin and from 0.119 to 0.642  $\mu\text{g/mL}$  for marbofloxacin. For the

resistant bacteria,  $EC_{50}$  estimates for S1 ranged from 1.81 to 13.38  $\mu\text{g}/\text{mL}$  for pradofloxacin and from 4.03 to 23.55  $\mu\text{g}/\text{mL}$  for marbofloxacin. For the less susceptible S2 population,  $EC_{50}$  values were 1.97 and 1.67-fold higher than the  $EC_{50}$  values of S1 for pradofloxacin and marbofloxacin, respectively.

The proportion of S1 (named F or distribution factor) was estimated as 0.99. When S1 was equal to the initial inoculum of  $5 \times 10^5$  CFU/mL, S2 was negligible ( $>1$  CFU/mL), but resistant mutants appeared when exposed to FQ concentrations lower than the MIC.

A good correlation was observed between the experimental and estimated MIC values in both FQs ( $R^2 = 0.986$  S1 and  $R^2 = 0.9887$  S2 for marbofloxacin,  $R^2 = 0.9975$  S1 and  $R^2 = 0.9973$  S2 for pradofloxacin) (Figure S17).

#### 2.4. Comparison of Predicted In Vivo Effects

*S. pseudintermedius*: Taking into account in vivo exposure to the recommended dosage regimen, the average drug killing effect ( $K_{\text{drug}}$ ) at steady state in a selected susceptible isolate (MRSP 41) was  $1.82 \text{ h}^{-1}$  (33 min) for marbofloxacin and  $2.21 \text{ h}^{-1}$  (27 min) for pradofloxacin. The average drug effect at steady state in a selected resistant isolate (MRSP 67) was  $0.08 \text{ h}^{-1}$  (750 min) for marbofloxacin and  $1.43 \text{ h}^{-1}$  (42 min) for pradofloxacin (Table 5). No differences in terms of killing effect were observed for marbofloxacin between the two assessed protein bindings (9.1% [22] and 25% [23]).

*S. aureus*: Taking into account in vivo exposure to the recommended dosage regimen for a selected susceptible isolate (MSSA B98), the time-average drug effect ( $K_{\text{drug}}$ ) at steady state was  $1.78 \text{ h}^{-1}$  (34 min) for marbofloxacin and  $2.15 \text{ h}^{-1}$  (28 min) for pradofloxacin. The average drug effect at steady state in a selected resistant isolate (MSSA B53) was  $0.0021 \text{ h}^{-1}$  (i.e., negligible) for marbofloxacin and  $0.28 \text{ h}^{-1}$  (214 min) for pradofloxacin (Table 5). No differences were observed for marbofloxacin between the two assessed protein binding values (9.1% [22] and 25% [23]).

*E. coli*: Taking into account in vivo exposure to the recommended dosage regimen for a selected susceptible isolate (*E. coli* 14L-1510), the time-average drug effect ( $K_{\text{drug}}$ ) at steady state was  $15.78 \text{ h}^{-1}$  (3.8 min) for marbofloxacin and  $8.23 \text{ h}^{-1}$  (7.3 min) for pradofloxacin. The average drug effect at steady state in a selected resistant isolate (*E. coli* 12L-2253) was  $0.0054 \text{ h}^{-1}$  (i.e., negligible) for marbofloxacin and  $0.11 \text{ h}^{-1}$  (545 min) for pradofloxacin (Table 5). No differences were observed for marbofloxacin between the two assessed protein binding values used (9.1% [22] and 25% [23]).

#### 2.5. Confirmation of PK/PD Index Target Value

*S. pseudintermedius*: For a typical susceptible bacterium, such as MRSP 41 (MIC marbofloxacin 0.18  $\mu\text{g}/\text{mL}$  and pradofloxacin 0.025  $\mu\text{g}/\text{mL}$ ), target  $fAUC_{\text{PK}_0-24\text{h}}/\text{MIC}$  values to achieve 90%  $E_{\text{max}}$  values were 35.9 and 35.7 h, corresponding to average free plasma concentrations of 0.26 and 0.037  $\mu\text{g}/\text{mL}$  for marbofloxacin and pradofloxacin, respectively (Table S9). No differences were observed for marbofloxacin between the two assessed protein binding values (9.1% [22] and 25% [23]).

*S. aureus*: For a typical susceptible bacterium, such as MSSA B98 (MIC marbofloxacin 0.35  $\mu\text{g}/\text{mL}$  and pradofloxacin 0.05  $\mu\text{g}/\text{mL}$ ), target  $fAUC_{\text{PK}_0-24\text{h}}/\text{MIC}$  values to achieve 90%  $E_{\text{max}}$  values were 31.7 and 44.9 h, corresponding to average free plasma concentrations of 0.46 and 0.094  $\mu\text{g}/\text{mL}$  for marbofloxacin and pradofloxacin, respectively (Table S9). No differences were observed for marbofloxacin between the two assessed protein binding values used (9.1% [22] and 25% [23]).

*E. coli*: For a typical susceptible bacterium, such as *E. coli* 14L-1510 (MIC marbofloxacin 0.35  $\mu\text{g}/\text{mL}$  and pradofloxacin 0.05  $\mu\text{g}/\text{mL}$ ), target  $fAUC_{\text{PK}_0-24\text{h}}/\text{MIC}$  values to achieve 90%  $E_{\text{max}}$  values were 26.9 and 26.3 h, corresponding to average free plasma concentrations of 0.028 and 0.024  $\mu\text{g}/\text{mL}$  for marbofloxacin and pradofloxacin, respectively (Table S6). No differences were observed for marbofloxacin between the two assessed protein bindings used (9.1% [22] and 25% [23]).

### 3. Discussion

This is the first study that compared two veterinary FQs used in veterinary dermatology using a PK/PD mathematical modelling approach. Our results showed that, at their licensed doses, the two investigated FQs do not show substantial differences in comparison with the predicted clinical efficacy against *S. pseudintermedius*, *S. aureus*, and susceptible *E. coli* collected from canine pyoderma. Moreover, as expected from the MIC measurements, TKC modelling showed that pradofloxacin is more potent than marbofloxacin (i.e., had lower  $EC_{50}$ ). However, their pharmacological efficacies measured from their maximum killing rates were similar. These two PD parameters generated from TKC analysis are not capable on their own of ranking these two antibiotics in terms of expected clinical efficiency. Thus, further integration into a PK/PD type index is necessary to obtain an overall assessment, which will take into account the administered doses and the internal exposure of the two drugs for the registered dosage regimen.

The main objective of the study was to compare two FQs used in veterinary dermatology, namely marbofloxacin and pradofloxacin. However, the findings from the study do not allow conclusions to be drawn on the use of the antibiotics in veterinary practice, for which randomised clinical trials represent the gold standard when comparing two antibiotics and their clinical outcome. These are not common in veterinary medicine, and, to our knowledge, clinical trials have not been conducted using these two antibiotics in the treatment of canine skin infections. It is therefore necessary to consider other surrogate criteria and to speculate on comparisons between the two antibiotics in terms of clinical efficacy. MIC is often implemented in these cases for the target pathogens. With regards to the two analysed FQs, pradofloxacin shows a much lower value in comparison with marbofloxacin, which could be erroneously interpreted as a clinical advantage. Indeed, MIC is only a hybrid variable that reflects standardised in vitro conditions of drug potency and efficacy and conclusions on the superiority of antibiotics in terms of clinical efficacy cannot be drawn from MIC comparison.

In this regards, it should be noted that the potency of a drug and its pharmacological efficacy are two pharmacological properties and that the efficacy measured under controlled in vitro conditions is only one of the elements that determines the overall clinical efficacy. Other factors determining clinical efficiency include the PK properties of the antibiotic and the selected dosage regimen.

Marbofloxacin and pradofloxacin were compared using a dynamic model that reproduced the in vivo plasma concentration profile obtained from licensed oral doses in dogs (2 and 3 mg/kg for marbofloxacin and pradofloxacin, respectively) in the test medium [16]. The author concluded that pradofloxacin possesses a greater bactericidal effect against both *S. pseudintermedius* and *S. aureus* in comparison with marbofloxacin. The results were attributable to higher  $fAUC_{24h}/MIC$  values resulting from pradofloxacin that had a more rapid decrease in the initial inoculum of  $5 \times 10^7$  CFU/mL. However, as mentioned in the Introduction section, this type of experimental protocol does not characterise the genuine pharmacodynamic properties of an antibiotic, and the results obtained are limited to single plasma concentration profiles, which have been reproduced for a given tested pathogen. Hence, our study aimed to quantify and characterize the main PD properties of marbofloxacin and pradofloxacin in order to predict their comparative efficiency. TKC assays are the most informative in vitro approach to estimate the PD properties of an antibiotic provided that the results obtained are modelled with a model in which potency and efficacy are explicitly estimable from the temporal dynamics of bactericidal activity. This is the case for the various semi-mechanistic models recently reviewed by Minichmayr et al. [8], and this is the first study that compared the PK/PD of marbofloxacin and pradofloxacin using TKC modelling.

$fAUC_{24h}/MIC$  has been widely adopted in the literature for all FQs, including marbofloxacin and pradofloxacin [24,25]. However, the values needed to achieve bacterial eradication and clinical efficacy have never been investigated in veterinary medicine. In humans, an  $fAUC_{24h}/MIC$  of 125 h is often reported following clinical data [25]. For

instance, an average free plasma concentration of a selected FQ over a 24-h dosing interval equal to 5 times the MIC should be recommended for therapeutic success. This leads to the selection of rather high doses of FQs, and alternative and more conservative lower index values have been proposed, in line with prudent use of veterinary antimicrobials as suggested by WHO guidelines [26]. Thus, achieving an  $fAUC_{24h}/MIC$  at 48 h makes it possible to reduce the dose by a factor of 2.6, in comparison with an  $fAUC_{24h}/MIC$  of 125 h. This can be achieved simply using the model that was developed to estimate PD parameters by replacing the static KC concentrations by the time course of free plasma concentrations expected for different dosing regimens. This approach allowed us to confirm that  $fAUC/MIC$  was the PK/PD index most predictive of the bactericidal effect for both drugs. In staphylococci, an  $fAUC_{24h}/MIC$  of approximately 25–45 h was necessary to achieve 90% of the in silico inhibitory effect in both susceptible and resistant isolates, which is in line with previously reported data from both in vivo and in vitro studies [24,25,27,28]. However, Lorenzutti et al. [12] showed that in *S. aureus*, a PK/PD index of at least 120 h is necessary to obtain 50% of the inhibitory effect when high inocula are used. This value, which is similar to the 125 h often recommended by default in human medicine, can be explained by the fact that high inocula already contain first-step mutant bacteria with a higher MIC. Thus, the likelihood of selecting subpopulations of first-step mutants is reduced by aiming for concentrations clearly higher than the MIC of the initial wild population. This is in line with results obtained in the murine thigh infection model of Ferran et al. [29], which demonstrated that the likelihood of resistance emergence to marbofloxacin is influenced by the inoculum size and pre-existing mutants before any antimicrobial treatments are administered. Likely for the same reason, the  $fAUC_{24h}/MIC$  values obtained from *E. coli* in our study are lower than those necessary to achieve a bacteriological cure at approximately 100–125 h and are obtained from human clinical trials or animal infection models. Indeed, ex vivo studies on veterinary FQs support that  $fAUC_{24h}/MIC$  values lower than 100 h can achieve bactericidal activity (3log<sub>10</sub> reduction) or total eradication in Gram-negative bacteria from pigs [30] or calves [31–33]. However, dynamic kill studies, which can mimic the drug effects in patients with immunosuppression or critical illnesses, have demonstrated with both human [34] and veterinary [35] FQs that  $fAUC_{24h}/MIC$  values lower than 100 h were associated with regrowth and/or resistance emergence.

Moreover, a review by Wright et al. [25] showed that  $fAUC_{24h}/MIC$  values of 30–35 h are necessary to achieve a clinical cure. It is relevant for veterinary medicine to note that for *S. pseudintermedius* and *S. aureus* did not show any reduced susceptibility within 24 h both in the presence and absence of FQs (pradofloxacin and marbofloxacin) [16].

The last element to be taken into consideration when comparing the two FQs relates to their PK properties and their dosage regimen as recommended in their marketing authorizations. It would have been advantageous to have had access to PK raw data (plasma concentrations) for both marbofloxacin and pradofloxacin of different origins and to reanalyse them with a non-linear mixed Effect Model (NLMEM) as previously shown with different class of antibiotics [7], despite the commercial sensitivities.

Considering the significant differences in clearance and plasma protein binding between the two substances and taking into account the recommended dosing regimens, it appears that the internal exposure to free concentrations of marbofloxacin under steady-state conditions was 2.4-fold higher than that of pradofloxacin with equilibrium free concentrations of 0.76 and 0.32 mg/L for marbofloxacin and pradofloxacin, respectively.

Future experiments should involve the acquisition of that information to propose a clinical breakpoint using Monte Carlo simulation. For instance, Yohannes et al. [15] used a PK/PD model to investigate whether intramuscular and intravenous doses of 2 mg/kg marbofloxacin were able to achieve adequate PK/PD indices necessary to obtain bacterial eradication in *S. pseudintermedius*, both in vitro and ex vivo (serum). PK/PD modelling resulting from real plasma concentrations, coupled with time-kill analysis, showed that the doses could not achieve the target AUC/MIC necessary to eradicate *S. pseudintermedius*; therefore, different dose regimens should be explored.

## 4. Materials and Methods

### 4.1. Selection of Bacterial Isolates and Antimicrobial Susceptibility

Twenty-four isolates obtained from cases of canine pyoderma were included in the study, comprising 8 *S. pseudintermedius*, 8 *S. aureus* and 8 *E. coli* isolates. We selected 1 pool of 4 marbofloxacin-susceptible isolates and 1 pool of 4 marbofloxacin-resistant isolates (Table S1). Resistant isolates were screened for chromosomal DNA gyrase (*gyrA*) and topoisomerase IV (*griA/parC*) mutations by PCR as previously described [36–38]. *E. coli* was also screened for plasmid-mediated quinolone resistance (PMQR) genes [39,40]. Susceptible isolates were considered as wild-type bacteria (WT) (Table S1). Equal proportions of methicillin susceptible (4 MSSA, 4 MSSP) and resistant (4 MRSA, 4 MRSP) staphylococcal isolates were selected.

### 4.2. MIC Measurement and Time-Kill Curve Technique

For the TKC study, MICs of marbofloxacin and pradofloxacin were initially obtained using the broth microdilution method according to CLSI guidelines [41]. Subsequently, a more accurate MIC measurement called “five series of overlapping dilutions” was adopted in this study. The method was developed by Aliabadi and Lees [42], and compared with the standard MIC measurement, it has the advantage of reducing the inaccuracy of the 2-fold MIC measurement from 100% to a maximum of 20%.

Isolates were thawed from storage in brain heart infusion (BHI, Oxoid, Basingstoke, UK) + 25% glycerol at  $-80\text{ }^{\circ}\text{C}$  and subcultured three times on blood agar to promote optimal growth according to CLSI guidelines [43]. MR isolates were subcultured two times on Mannitol salt agar (Oxoid, Basingstoke, UK) + 6 mg/L oxacillin (MS+) and subsequently on BA to ensure that methicillin resistance (MR) was preserved. Bacterial density was adjusted to equivalence with 0.5 McFarland standard (approx.  $1\text{--}2 \times 10^8$  CFU/mL) using DensiCheck<sup>®</sup> (Biomérieux, Marcy L'Étoile, France) and diluted 100-fold to achieve a  $10^6$  CFU/mL final suspension. Then, 50  $\mu\text{L}$  of bacterial suspension was added to each well of a 96-well plate containing 50  $\mu\text{L}$  of prewarmed FQ-containing cation-adjusted Mueller-Hinton broth (CAMHB, Merck, Steinheim, Germany) to yield a final inoculum of  $5 \times 10^5$  CFU/mL exposed to 0 $\times$ , 0.5 $\times$ , 1 $\times$ , 2 $\times$ , 4 $\times$  and 8 $\times$  of the MIC. Plates were incubated at 37  $^{\circ}\text{C}$  for 24 h. At 0, 0.5, 1, 2, 4, 8 and 24 h of incubation, 25  $\mu\text{L}$  from each of the wells was serially 10-fold diluted with phosphate-buffered saline (PBS, Fisher, Geel, Belgium) up to  $10^{-8}$ . After dilution, 25  $\mu\text{L}$  spots were applied onto square petri dishes containing Mueller-Hinton agar (MHA, Merck, Steinheim, Germany), left to dry in a microbiology cabinet and then incubated at for 16–24 h at 37  $^{\circ}\text{C}$ . After incubation, cell counts expressed in CFU/mL were back calculated from the lowest dilution with approximately 3–30 CFU per spot. The limit of enumeration, defined as the lowest number of countable cells, was set at 40 CFU/mL (one or no colonies in a 25  $\mu\text{L}$  spot at the lowest dilution). Each experiment was conducted in duplicate on separate days.

Results were  $\log_{10}$  transformed and plotted with time (h) on the x axis and bacterial count (CFU/mL) on the y axis.

### 4.3. Pharmacodynamic Data Analysis and Modelling

Data from TKCs were analysed using the Phoenix 8.3.0.5005 software package (Certara, Princeton, NJ, USA). A semi-mechanistic model proposed by Nielsen and Frieberg [19] was initially adopted for this study. The model included two compartments: the “S” containing susceptible bacteria, and a second compartment “P”, containing persisters, which are non-growing and drug-insensitive bacteria (Figure 1).

Mathematical modelling, including a bacterial growth model, drug effect and secondary parameters (MICs), were obtained following a method previously described by Pelligand et al. [44] (Text S1).

#### 4.4. Pre-Existing Heterogenous Population Model

Since the initial model proposed by Nielsen and Friberg [19] did not capture the regrowth of *E. coli* exposed to  $1 \times \text{MIC}$ , we hypothesised that pre-existing first-step mutants were present within the total population of *E. coli*, as described by Campion et al. [20]. The ratio between first-step mutants and the total bacterial population has been shown to be approximately  $10^{-8}$  to  $10^{-9}$  based on growth curves [34]. Thus, we concluded that the initial population (starting inoculum) consisted of two subpopulations, representing a heterogenous bacterial population with a proportion (F1) of bacteria being a highly susceptible dominant population (S1) and the remaining sub-dominant population (S2) having a lower susceptibility. F1 was estimated by the model illustrated in Figure 2 and as shown by Mead et al. [11].

#### 4.5. Covariate Analyses

To allow for parameter adjustment in relation to the initial FQ susceptibility of isolates (resistant versus non-resistant), a binary categorical covariate was tested during PD parameters estimation for system parameters common to both drugs (e.g.,  $K_{\text{growthmax}}$ , alpha, and  $B_{\text{max}}$ ) or drug-specific parameters for each drug ( $E_{\text{max}}$ ,  $\text{EC}_{50}$ , and gamma). Selection of significant covariate effects was carried out using the Stepwise Phoenix tool. It involved stepwise forward and backward parallelized addition and deletion of covariate effects. Covariates were added progressively to determine if the goodness of fit improved compared to a predefined threshold in objective function value (OFV). In this case, the Bayesian information criterion (BIC) with thresholds of 6.635 and 10.828 points was used to add and remove a covariate, respectively. The covariate analysis was carried out to elucidate the origin of variability of resistant or susceptible isolates; hence, resistance vs susceptible was considered as a factor rather than a covariate.

#### 4.6. Comparison of In Vivo Drug Effects Predicted from Licensed Dosage Regimens

Plasma concentration time curves were obtained using the Unscan it software (version 7.0, Silk Scientific, Provo, UT, USA) from the previously published PK studies where dogs received 2 mg/kg marbofloxacin [18] or 3 mg/kg pradofloxacin [21] (Table S2). Non-compartmental analysis was carried out on free plasma concentrations in Phoenix<sup>®</sup> NLME<sup>®</sup> Protein, and binding of 36% [45] was considered for pradofloxacin. For marbofloxacin two different protein bindings (9.1% from product monograph [22] and 25% Bregante et al. [23]) were explored. The PK parameters are presented in Table S2 ( $C_{\text{max}}$ ,  $T_{\text{max}}$ , half-life, clearance and  $\text{AUC}_{0-24\text{h}}$  and  $\text{AUC}_{0-\text{infinity}}$ ). The average plasma concentrations after the first dose and at steady state were calculated by dividing the corresponding AUC ( $\text{AUC}_{0-24\text{h}}$  and  $\text{AUC}_{0-\text{infinity}}$ , respectively) by 24 h [46].

Time-averaged drug effects ( $K_{\text{drug}}, \text{h}^{-1}$ ) were computed from the Hill's equation (Text S1, Equation (2)) and these average daily free concentrations to compare predicted in vivo effects ( $K_{\text{drug}}$ ) between FQs for each bacterial species (susceptible and resistant).

#### 4.7. In Silico Dose Fractionation Experiments

We performed an in silico dose fractionation to confirm the nature of the best PK/PD index ( $f\text{AUC}_{\text{PK}_0-24\text{h}}/\text{MIC}$  or  $\%fT > \text{MIC}$ ) by simulating the bacteriological response to a wide range of escalating dosing regimens in order to achieve no effect or maximum effects. In total, 12 escalating doses (including control curve which corresponds to no antibiotics administered) were included and administered:

- As a single dose over 24 h
- Split in 2 half-doses, given every 12 h
- Split in 4 quarter-doses, given every 6 h

Similar to the predicted drug effect, two different protein bindings of marbofloxacin were taken into account.

This yielded a total of 34 dosage regimens for which we computed the area under the free FQ concentration curve over the MIC ( $fAUC_{PK\_0-24h}/MIC$ ) and the percentage of time the free concentration exceeded the MIC ( $\%fT > MIC$ ). Effects on bacterial inoculum were evaluated up to 24 h, and the area under the bacterial concentration curve ( $AUC_{bact-24h}$ ) was computed. The bacterial count was set to 0 (eradication) as soon as the bacterial concentration reached the LOQ of the enumeration method (40 CFU/mL).

An inhibitory effect sigmoid PD model ( $I_{max}$ ) was implemented to fit the PK/PD index ( $\%fT > MIC$  and  $fAUC_{0-24h}/MIC$ ) versus  $AUC_{bact-24h}$ . The  $I_{max}$  model describes the inhibitory effect of a drug according to the following formula (Equation (1)):

$$\text{Effect} = E_0 - \frac{(I_{max} \times \text{index}^{\text{slope}})}{(\text{index}^{\text{slope}} + \text{index}_{50}^{\text{slope}})} \quad (1)$$

Here, effect (the observed effect),  $E_0$ , and  $I_{max}$  are expressed in terms of  $\text{Log}_{10}AUC_{bact0-24h}$ . Specifically,  $E_0$  represents the maximal effect obtained for the control curve,  $I_{max}$  the amplitude of the maximal inhibitory effect, and  $E_0 - I_{max}$  represents the maximal possible inhibitory observed effect.  $\text{Index}_{50}$  is the magnitude of the PK/PD index ( $\%fT > MIC$  or  $fAUC_{0-24h}/MIC$ ) that achieves 50% of  $I_{max}$ , and slope is the steepness of the sigmoid curve. The best PK/PD index that predicted the bactericidal effect was assessed by regression analysis ( $R^2$ ), Akaike index criterion (AIC), and visual inspection of graphs (Figure 3). Moreover,  $\text{Index}_{90\%}$  was calculated as the breakpoint value for the PK/PD index, which allowed calculation of the average free plasma concentration required over 24 h to achieve 90% of the maximal efficacy.

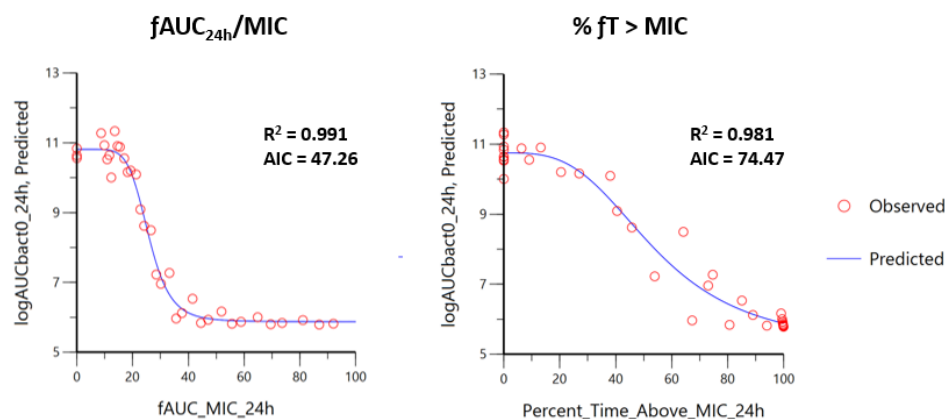


**Figure 3.** Comparison of fitting for prediction of  $\log_{10}AUC_{bact0-24h}$  (y axis) obtained from the  $I_{max}$  model, and  $fAUC_{24h}/MIC$  ((left plot), x axis) or  $\%fT > MIC$  ((right plot), x axis) in a selected isolate (MRSP 41) with an marbofloxacin MIC of 0.25  $\mu\text{g}/\text{mL}$ .  $R^2$  is the coefficient of determination providing the percentage of variance explained by the model. AIC is the Akaike information criterion, which represents a measure of goodness of fit. In this case,  $fAUC_{24h}/MIC$  represents the best PK/PD index with the highest  $R^2$  and the lowest AIC.

## 5. Conclusions

When recommended doses, clearance, and protein binding differences are considered, we estimated that pradofloxacin may have a higher drug effect than marbofloxacin in some situations. However, the limitation of TCKs relies on static concentrations over time, which cannot capture the time course of drug concentrations during antimicrobial treatment.

For all the three bacterial species investigated in the study, the predicted clinical outcome relies on  $fAUC/MIC$ , which is dependent on drug exposure to achieve bacterial eradication. However, when comparing the predicted clinical efficacy between the two FQs, no substantial differences were observed in the susceptible isolates that are of concern in clinical settings.

The advantage of pradofloxacin depends on its narrow mutant selection window (MSW), which should limit the time during which target drug concentrations are likely to select for first-step mutants. To explore this hypothesis, further investigations on the resistance emergence and optimal dosing regimens should be implemented with dynamic kill studies (e.g., hollow fibre infection model) and randomised blinded clinical trials to predict and achieve complete bacteriological eradication, together with the reduction of resistance emergence.

**Supplementary Materials:** The following supporting information can be downloaded at: <https://www.mdpi.com/article/10.3390/antibiotics12101548/s1>, Table S1: List of isolates; Table S2: PK data; Table S3: PD data *S. pseudintermedius*; Table S4: PD data *S. aureus*; Table S5: PD data *E. coli*; Table S6: Secondary parameters *S. pseudintermedius*; Table S7: Secondary parameters *S. aureus*; Table S8: Secondary parameters *E. coli*; Table S9: Critical PK/PD values; Figures S1–S12 Visual predictive checks (VPC); Figures S13–S15: Predicted (IPRED) vs observed bacterial counts (DV); Figure S16: Conditional (CWRES) and individual (IWRES) weighted residuals vs predicted bacterial count (PRED); Figure S17: Correlation between experimental and model-estimated MICs; Text S1: Mathematical modelling. References [47–52] are only cited in Supplementary Materials.

**Author Contributions:** Conceptualization, S.A. and L.P.; methodology, S.A., L.P., P.-L.T. and A.M.; software, S.A., L.P. and A.M.; validation, S.A., L.P., A.M. and P.-L.T.; formal analysis, S.A. and L.P.; investigation, S.A. and L.P.; resources, S.A. and L.P.; data curation, S.A., L.P. and P.-L.T.; writing—original draft preparation, S.A., L.P., A.M. and R.B.; writing—review and editing, S.A., L.P., A.M., P.-L.T. and R.B.; supervision, L.P. and R.B.; project administration, L.P.; funding acquisition, L.P. and R.B. All authors have read and agreed to the published version of the manuscript.

**Funding:** This research was funded by the Veterinary Medicine Directorate, grant number VM0536.

**Institutional Review Board Statement:** Not applicable.

**Informed Consent Statement:** Not applicable.

**Data Availability Statement:** The data presented in this study are available on request from the corresponding author.

**Acknowledgments:** We thank Anette Loeffler (Royal Veterinary College, London) for providing staphylococcal isolates and Dorina Timofte and Flavia Zendri (University of Liverpool) for providing *E. coli* isolates. We also thank Bayer Animal Health (Monheim, Germany) for kindly providing pradofloxacin powder.

**Conflicts of Interest:** The authors declare no conflict of interest. The funders had no role in the design of the study; in the collection, analyses, or interpretation of data; in the writing of the manuscript; or in the decision to publish the results.

## References

1. EUCAST. European Committee on Antimicrobial Susceptibility Testing. 2023. Available online: [https://www.eucast.org/fileadmin/src/media/PDFs/EUCAST\\_files/Breakpoint\\_tables/v\\_13.0\\_Breakpoint\\_Tables.pdf](https://www.eucast.org/fileadmin/src/media/PDFs/EUCAST_files/Breakpoint_tables/v_13.0_Breakpoint_Tables.pdf) (accessed on 1 July 2023).
2. Andrews, J.M. Determination of minimum inhibitory concentrations. *J. Antimicrob. Chemother.* **2001**, *48*, 5–16. [[CrossRef](#)] [[PubMed](#)]
3. Mouton, J.W.; Muller, A.E.; Canton, R.; Giske, C.G.; Kahlmeter, G.; Turnidge, J. MIC-based dose adjustment: Facts and fables. *J. Antimicrob. Chemother.* **2018**, *73*, 564–568. [[CrossRef](#)] [[PubMed](#)]
4. Jacobs, M.; Grégoire, N.; Couet, W.; Bulitta, J.B. Distinguishing antimicrobial models with different resistance mechanisms via population pharmacodynamic modeling. *PLoS Comput. Biol.* **2016**, *12*, e1004782. [[CrossRef](#)]
5. Toutain, P.L.; Pelligand, L.; Lees, P.; Bousquet-Mélou, A.; Ferran, A.A.; Turnidge, J.D. The pharmacokinetic/pharmacodynamic paradigm for antimicrobial drugs in veterinary medicine: Recent advances and critical appraisal. *J. Vet. Pharmacol. Ther.* **2021**, *44*, 172–200. [[CrossRef](#)]
6. Foerster, S.; Unemo, M.; Hathaway, L.J.; Low, N.; Althaus, C.L. Time-kill curve analysis and pharmacodynamic modelling for in vitro evaluation of antimicrobials against *Neisseria gonorrhoeae*. *BMC Microbiol.* **2016**, *16*, 216. [[CrossRef](#)] [[PubMed](#)]
7. Pelligand, L.; Lees, P.; Sidhu, P.K.; Toutain, P.-L. Semi-mechanistic modeling of florfenicol time-kill curves and in silico dose fractionation for calf respiratory pathogens. *Front. Microbiol.* **2019**, *10*, 1237. [[CrossRef](#)] [[PubMed](#)]
8. Minichmayr, I.K.; Aranzana-Climent, V.; Friberg, L.E. Pharmacokinetic/pharmacodynamic models for time courses of antibiotic effects. *Int. J. Antimicrob. Agents* **2022**, *60*, 106616. [[CrossRef](#)]



9. Regoes, R.R.; Wiuff, C.; Zappala, R.M.; Garner, K.N.; Baquero, F.; Levin, B.R. Pharmacodynamic functions: A multiparameter approach to the design of antibiotic treatment regimens. *Antimicrob. Agents Chemother.* **2004**, *48*, 3670–3676. [CrossRef]
10. Toutain, P.-L.; Bousquet-Mélou, A.; Damborg, P.; Ferran, A.A.; Mevius, D.; Pelligand, L.; Veldman, K.T.; Lees, P. En route towards European clinical breakpoints for veterinary antimicrobial susceptibility testing: A position paper explaining the VetCAST approach. *Front. Microbiol.* **2017**, *8*, 2344. [CrossRef]
11. Mead, A.; Toutain, P.-L.; Richez, P.; Pelligand, L. Quantitative Pharmacodynamic Characterization of Resistance versus Heteroresistance of Colistin in *E. coli* Using a Semimechanistic Modeling of Killing Curves. *Antimicrob. Agents Chemother.* **2022**, *66*, e00793–22. [CrossRef]
12. Lorenzutti, A.M.; San Andrés-Larrea, M.I.; Fernández-Varón, E.; Zarazaga, M.d.P.; Molina-López, A.M.; Serrano-Rodríguez, J.M. Effects of Growth Medium and Inoculum Size on Pharmacodynamics Activity of Marbofloxacin against *Staphylococcus aureus* Isolated from Caprine Clinical Mastitis. *Antibiotics* **2021**, *10*, 1290. [CrossRef] [PubMed]
13. Blondeau, J.M.; Shebelski, S.D. Comparative in vitro killing of canine strains of *Staphylococcus pseudintermedius* and *Escherichia coli* by cefovecin, cefazolin, doxycycline and pradofloxacin. *Vet. Dermatol.* **2016**, *27*, 267–e63. [CrossRef] [PubMed]
14. Blondeau, J.M.; Fitch, S.D. In vitro killing of canine strains of *Staphylococcus pseudintermedius* and *Escherichia coli* by cefazolin, cefovecin, doxycycline and pradofloxacin over a range of bacterial densities. *Vet. Dermatol.* **2020**, *31*, 187–e39. [CrossRef] [PubMed]
15. Yohannes, S.; Awji, E.G.; Lee, S.-J.; Park, S.-C. Pharmacokinetics and pharmacokinetic/pharmacodynamic integration of marbofloxacin after intravenous and intramuscular administration in beagle dogs. *Xenobiotica* **2015**, *45*, 264–269. [CrossRef] [PubMed]
16. Körber-Irrgang, B.; Wetzstein, H.G.; Bagel-Trah, S.; Hafner, D.; Kresken, M. Comparative activity of pradofloxacin and marbofloxacin against coagulase-positive staphylococci in a pharmacokinetic–pharmacodynamic model based on canine pharmacokinetics. *J. Veter. Pharmacol. Ther.* **2012**, *35*, 571–579. [CrossRef]
17. Boothe, D.M.; Bush, K.M.; Boothe, H.W.; Davis, H.A. Pharmacokinetics and pharmacodynamics of oral pradofloxacin administration in dogs. *Am. J. Veter-Res.* **2018**, *79*, 1268–1276. [CrossRef]
18. Schneider, M.; Thomas, V.; Boisrame, B.; Deleforge, J. Pharmacokinetics of marbofloxacin in dogs after oral and parenteral administration. *J. Vet. Pharmacol. Ther.* **1996**, *19*, 56–61. [CrossRef]
19. Nielsen, E.I.; Friberg, L.E. Pharmacokinetic-pharmacodynamic modeling of antibacterial drugs. *Pharmacol. Rev.* **2013**, *65*, 1053–1090. [CrossRef]
20. Champion, J.J.; McNamara, P.J.; Evans, M.E. Pharmacodynamic modeling of ciprofloxacin resistance in *Staphylococcus aureus*. *Antimicrob. Agents Chemother.* **2005**, *49*, 209–219. [CrossRef]
21. Hauschild, G.; Rohn, K.; Engelhardt, E.; Sager, M.; Harges, J.; Gosheger, G. Pharmacokinetic study on pradofloxacin in the dog—Comparison of serum analysis, ultrafiltration and tissue sampling after oral administration. *BMC Vet. Res.* **2013**, *9*, 32. [CrossRef]
22. Zeniquin®. Product Monograph. Available online: [https://www2.zoetisus.com/content/\\_assets/docs/vmips/package-inserts/zeniquin.pdf](https://www2.zoetisus.com/content/_assets/docs/vmips/package-inserts/zeniquin.pdf) (accessed on 1 July 2023).
23. Bregante, M.A.; de Jong, A.; Aramayona, J.J.; Garcia, M.A.; Solans, C.; Rueda, S. Protein binding of fluoroquinolones applied to live stock and companion animals. In Proceedings of the 8th International Congress European Association for Veterinary Pharmacology and Toxicology (EAVPT), Jerusalem, Israel, 30 July–3 August 2000; p. 88.
24. Papich, M.G. Pharmacokinetic–pharmacodynamic (PK–PD) modeling and the rational selection of dosage regimes for the prudent use of antimicrobial drugs. *Vet. Microbiol.* **2014**, *171*, 480–486. [CrossRef] [PubMed]
25. Wright, D.H.; Brown, G.H.; Peterson, M.L.; Rotschafer, J.C. Application of fluoroquinolone pharmacodynamics. *J. Antimicrob. Chemother.* **2000**, *46*, 669–683. [CrossRef] [PubMed]
26. WHO. World Health Organisation. 2023. Available online: <https://www.who.int/news-room/fact-sheets/detail/antimicrobial-resistance> (accessed on 1 July 2023).
27. Drusano, G.L. Pharmacokinetics and pharmacodynamics of antimicrobials. *Clin. Infect. Dis.* **2007**, *45*, S89–S95. [CrossRef]
28. Broussou, D.C.; Toutain, P.-L.; Woehrlé, F.; El Garch, F.; Bousquet-Melou, A.; Ferran, A.A. Comparison of in vitro static and dynamic assays to evaluate the efficacy of an antimicrobial drug combination against *Staphylococcus aureus*. *PLoS ONE* **2019**, *14*, e0211214. [CrossRef] [PubMed]
29. Ferran, A.; Dupouy, V.; Toutain, P.-L.; Bousquet-Mélou, A. Influence of inoculum size on the selection of resistant mutants of *Escherichia coli* in relation to mutant prevention concentrations of marbofloxacin. *Antimicrob. Agents Chemother.* **2007**, *51*, 4163–4166. [CrossRef] [PubMed]
30. Wang, J.; Hao, H.; Huang, L.; Liu, Z.; Chen, D.; Yuan, Z. Pharmacokinetic and pharmacodynamic integration and modeling of enrofloxacin in swine for *Escherichia coli*. *Front. Microbiol.* **2016**, *7*, 36. [CrossRef]
31. Potter, T.; Illambas, J.; Pelligand, L.; Rycroft, A.; Lees, P. Pharmacokinetic and pharmacodynamic integration and modelling of marbofloxacin in calves for *Mannheimia haemolytica* and *Pasteurella multocida*. *Vet. J.* **2013**, *195*, 53–58. [CrossRef]
32. Illambas, J.; Potter, T.; Cheng, Z.; Rycroft, A.; Fishwick, J.; Lees, P. Pharmacodynamics of marbofloxacin for calf pneumonia pathogens. *Res. Vet. Sci.* **2013**, *94*, 675–681. [CrossRef]
33. AliAbadi, F.S.; Lees, P. Pharmacokinetics and pharmacokinetic/pharmacodynamic integration of marbofloxacin in calf serum, exudate and transudate. *J. Vet. Pharmacol. Ther.* **2002**, *25*, 161–174. [CrossRef]
34. Singh, R.; Ledesma, K.R.; Chang, K.-T.; Hou, J.-G.; Prince, R.A.; Tam, V.H. Pharmacodynamics of moxifloxacin against a high inoculum of *Escherichia coli* in an in vitro infection model. *J. Antimicrob. Chemother.* **2009**, *64*, 556–562. [CrossRef]

35. Gebru, E.; Choi, M.-J.; Lee, S.-J.; Damte, D.; Park, S.C. Mutant-prevention concentration and mechanism of resistance in clinical isolates and enrofloxacin/marbofloxacin-selected mutants of *Escherichia coli* of canine origin. *J. Med. Microbiol.* **2011**, *60*, 1512–1522. [CrossRef] [PubMed]
36. Kim, H.B.; Park, C.H.; Kim, C.J.; Kim, E.-C.; Jacoby, G.A.; Hooper, D.C. Prevalence of plasmid-mediated quinolone resistance determinants over a 9-year period. *Antimicrob. Agents Chemother.* **2009**, *53*, 639–645. [CrossRef] [PubMed]
37. Intorre, L.; Vanni, M.; Di Bello, D.; Pretti, C.; Meucci, V.; Tognetti, R.; Soldani, G.; Cardini, G.; Jousson, O. Antimicrobial susceptibility and mechanism of resistance to fluoroquinolones in *Staphylococcus intermedius* and *Staphylococcus schleiferi*. *J. Vet. Pharmacol. Ther.* **2007**, *30*, 464–469. [CrossRef] [PubMed]
38. Schmitz, F.-J.; Jones, M.E.; Hofmann, B.; Hansen, B.; Scheuring, S.; Lückefahr, M.; Fluit, A.; Verhoef, J.; Hadding, U.; Heinz, H.-P. Characterization of *griA*, *griB*, *gyrA*, and *gyrB* mutations in 116 unrelated isolates of *Staphylococcus aureus* and effects of mutations on ciprofloxacin MIC. *Antimicrob. Agents Chemother.* **1998**, *42*, 1249–1252. [CrossRef]
39. Robicsek, A.; Strahilevitz, J.; Sahm, D.F.; Jacoby, G.A.; Hooper, D.C. qnr prevalence in ceftazidime-resistant Enterobacteriaceae isolates from the United States. *Antimicrob. Agents Chemother.* **2006**, *50*, 2872–2874. [CrossRef]
40. Ciesielczuk, H.; Hornsey, M.; Choi, V.; Woodford, N.; Wareham, D.W. Development and evaluation of a multiplex PCR for eight plasmid-mediated quinolone-resistance determinants. *J. Med. Microbiol.* **2013**, *62*, 1823–1827. [CrossRef]
41. *CLSI-VET01-A4*; Performance Standards for Antimicrobial Disk and Dilution Susceptibility Tests for Bacteria Isolated From Animals: Approved Standard. 4th ed. Clinical and Laboratory Standards Institute: Wayne, PA, USA, 2013.
42. Aliabadi, F.S.; Lees, P. Pharmacokinetics and pharmacodynamics of danofloxacin in serum and tissue fluids of goats following intravenous and intramuscular administration. *Am. J. Vet. Res.* **2001**, *62*, 1979–1989. [CrossRef]
43. *CLSI-M26-A*; M26-A: Methods for Determining Bactericidal Activity of Antimicrobial Agents; Approved Guideline. Clinical and Laboratory Standards Institute: Wayne, PA, USA, 1999.
44. Azzariti, S.; Bond, R.; Loeffler, A.; Zendri, F.; Timofte, D.; Chang, Y.-M.; Pelligand, L. Investigation of In Vitro Susceptibility and Resistance Mechanisms in Skin Pathogens: Perspectives for Fluoroquinolone Therapy in Canine Pyoderma. *Antibiotics* **2022**, *11*, 1237. [CrossRef]
45. Bregante, M.A.; De Jong, A.; Calvo, A.; Hernandez, E.; Rey, R.; Garcia, M.A. Protein binding of pradofloxacin, a novel 8-cyanofluoroquinolone, in dog and cat plasma. *J. Vet. Pharmacol. Ther.* **2003**, *26*, 87–88.
46. Toutain, P.-L.; Bousquet-mélou, A. Plasma terminal half-life. *J. Vet. Pharmacol. Ther.* **2004**, *27*, 427–439. [CrossRef]
47. *CLSI-VET01S*; Performance Standards for Antimicrobial Disk and Dilution Susceptibility Tests for Bacteria Isolated From Animals. 5th ed. Clinical and Laboratory Standards Institute: Wayne, PA, USA, 2020.
48. Marbocyl®. Product Monograph. Available online: <https://www.noahcompendium.co.uk/?id=-459540> (accessed on 1 July 2023).
49. Nielsen, E.I.; Cars, O.; Friberg, L.E. Pharmacokinetic/pharmacodynamic (PK/PD) indices of antibiotics predicted by a semimechanistic PKPD model: A step toward model-based dose optimization. *Antimicrob. Agents Chemother.* **2011**, *55*, 4619–4630. [CrossRef] [PubMed]
50. Nielsen, E.I.; Viberg, A.; Löwdin, E.; Cars, O.; Karlsson, M.O.; Sandström, M. Semimechanistic pharmacokinetic/pharmacodynamic model for assessment of activity of antibacterial agents from time-kill curve experiments. *Antimicrob. Agents Chemother.* **2007**, *51*, 128–136. [CrossRef] [PubMed]
51. Khan, D.D.; Lagerbäck, P.; Cao, S.; Lustig, U.; Nielsen, E.I.; Cars, O.; Hughes, D.; Andersson, D.I.; Friberg, L.E. A mechanism-based pharmacokinetic/pharmacodynamic model allows prediction of antibiotic killing from MIC values for WT and mutants. *J. Antimicrob. Chemother.* **2015**, *70*, 3051–3060. [CrossRef] [PubMed]
52. Mouton, J.W.; Vinks, A.A. Relationship between minimum inhibitory concentration and stationary concentration revisited: Growth rates and minimum bactericidal concentrations. *Clin. Pharmacokinet.* **2005**, *44*, 767–769. [CrossRef] [PubMed]

**Disclaimer/Publisher’s Note:** The statements, opinions and data contained in all publications are solely those of the individual author(s) and contributor(s) and not of MDPI and/or the editor(s). MDPI and/or the editor(s) disclaim responsibility for any injury to people or property resulting from any ideas, methods, instructions or products referred to in the content.